Massive Star Birth: A Crossroads of Astrophysics
Proceedings IAU Symposium No. 227, 2005
R. Cesaroni, M. Felli, E. Churchwell & C. M. Walmsley, eds.

doi:10.1017/S1743921305004382

Centrally condensed turbulent cores: massive stars or fragmentation

Clare L. Dobbs† and Ian A. Bonnell

School of Physics and Astronomy, University of St Andrews, North Haugh, St Andrews, Fife, KY16 9SS, UK
email:cld2@st-and.ac.uk

Abstract. We present numerical investigations into the formation of massive stars from turbulent cores of density gradient $\rho \propto r^{-1.5}$. The results of five hydrodynamical simulations are described, following the collapse of the core, fragmentation and the formation of small clusters of protostars. We generate two different initial turbulent velocity fields corresponding to power-law spectra $P \propto k^{-4}$ and $P \propto k^{-3.5}$, and apply two different initial core radii. Calculations are included for both completely isothermal collapse, and a non-isothermal equation of state above a critical density (10^{-14}gcm^{-3}). Our calculations reveal the preference of fragmentation over monolithic star formation in turbulent cores. Fragmentation was prevalent in all the isothermal cases. Although disc fragmentation was largely suppressed in the non-isothermal runs due to the small dynamic range between the initial density and the critical density, our results show that some fragmentation still persisted. This is inconsistent with previous suggestions that turbulent cores result in the formation of a single massive star. We conclude that turbulence cannot be measured as an isotropic pressure term.

Keywords. hydrodynamics, turbulence, stars:formation

1. Introduction

The contents of these proceedings are also described in Dobbs, Bonnell & Clark (2005).

There are several potential difficulties in forming high-mass stars. Firstly, the radiation pressure from a high-mass star is sufficient to reverse the infall of gas (Wolfire & Casinelli 1987) and prevent further accretion. Secondly, the timescale of less than 10^6 years to accumulate 10 to more than 100 $M_\odot$ implies large accretion rates (Zinnecker, McCaughrean & Wilking 1993). Finally the crowded location of massive stars in the centre of clusters (Clarke, Bonnell, & Hillenbrand 2000, Hillenbrand & Hartmann 1998, Carpenter, Meyer *et al.* 1997, Lada & Lada 2003) limits the final mass of any collapsing fragment (Zinnecker, McCaughrean & Wilking 1993, Bonnell, Bate & Zinnecker 1998. Various suggestions have been proposed to overcome these difficulties. Accretion could occur preferentially through an equatorial disc, whilst most radiation is emitted towards the poles (Yorke & Sonnhalter 2002). Alternatively, radiation pressure could be overwhelmed by ultra-high accretion rates (McKee & Tan 2003). Thirdly, massive stars could form due to stellar mergers in the ultra-dense core of a cluster (Bonnell, Bate & Zinnecker 1998, Bonnell & Bate 2002.

The McKee & Tan (2003), McKee & Tan (2002) model depends on high accretion rates that would be expected to occur in a dense gas core in the centre of a cluster. This core is envisioned to be supported by turbulence, as thermal pressure is inadequate, and centrally condensed in order to prevent fragmentation. Even neglecting how such a core could arise in the centre of a stellar cluster, one potential difficulty is that turbulent

† Present address: School of Physics and Astronomy, University of St Andrews, North Haugh, St Andrews, Fife, KY16 9SS

clouds are known for their tendency to fragment and form a stellar cluster. We present calculations adopting a centrally condensed turbulent core of a density and velocity dispersion comparable to McKee & Tan (2002). The purpose of our work is to investigate whether the centrally condensed conditions assumed by McKee and Tan are sufficient to prevent fragmentation and consequently provide a suitable approach to massive star formation.

2. Computational Method

We use the 3D smoothed particle hydrodynamics (SPH) code to perform simulations with 10^6 particles. The insertion of sink particles is used to extend calculations. All computations were performed using the United Kingdom's Astrophysical Fluids Facility (UKAFF), a 128 CPU SGI Origin 3000 supercomputer.

2.1. *Initial conditions*

McKee & Tan (2003) assume a centrally condensed core, following a density profile of $\rho \propto r^{-k_\rho}$. We take $k_\rho = 1.5$, the fiducial value of McKee & Tan (2003).

The core radius was chosen as either 0.06pc (central density $\sim 3 \times 10^{-15}\mathrm{gcm}^{-3}$) or 0.2 pc (central density $2 \times 10^{-16}\mathrm{gcm}^{-3}$) with a mass of $30M_\odot$. McKee & Tan (2003) use similar initial conditions, but take a mass of $60M_\odot$ to form a $30M_\odot$ star with 50% efficiency. Results are described in terms of the free fall time, $\sim 4.5 \times 10^4$ years for the 0.06pc core and 2.7×10^5 years for the 0.2pc core.

An isothermal equation of state was chosen for 3 simulations, which vary the core radius and turbulent power spectrum (Section 2.1.1). Two calculations were then repeated with a non isothermal equation of state above a critical density: $P \propto \rho^\gamma$ where $\gamma = 1$ for $\rho < 10^{-14}\mathrm{gcm}^{-3}$ and $\gamma = 1.67$ for $\rho \geqslant 10^{-14}\mathrm{gcm}^{-3}$.

2.1.1. *Turbulence*

McKee & Tan (2003) incorporate turbulence by means of an effective turbulent pressure term whereby $P \propto r^{-k_P}$. Taking $k_\rho = 1.5$, their analysis leads to a velocity size-scale relation $\sigma \propto r^{0.25}$, where σ is the velocity dispersion. This is shallower than observational results obtained for the similar Larson relation $\sigma \propto L^\alpha$ (L a typical length scale), in which $0.25 < \alpha < 0.75$, e.g. $\alpha = 0.38$ (Larson 1981), $\alpha = 0.5$ (Myers 1983).

We simulate turbulence by sampling from a Gaussian with power spectrum

$$P(k) \equiv \langle |v_k| \rangle^2 \propto k^{-n}, \tag{2.1}$$

where k is the wavenumber. This method is described more fully in Dobbs, Bonnell & Clark (2005), but overall generates a velocity field containing a velocity size-scale relation similar to the Larson relation. Calculations are included for $\sigma \propto r^{0.25}$, consistent with McKee & Tan (2003), and $\sigma \propto r^{0.5}$ which corresponds better with observations.

The core is initially in virial equilibrium. The ratios of turbulent to gravitational energy are $E_{turb}/E_{grav} \sim 0.4$ for $R = 0.06pc$ and $E_{turb}/E_{grav} \sim 0.25$ for $R = 0.2pc$. The turbulent energy is then allowed to dissipate over the dynamical timescale of the core (Mac Low, Klessen *et al.* 1997).

https://doi.org/10.1017/S1743921305004382 Published online by Cambridge University Press

3. Results

A summary of the calculations undertaken, their parameters and the overall results are shown in Table 1. The parameter α describes the initial velocity dispersion (where $\sigma \propto r^{\alpha}$).

In all simulations, turbulence initially supports the core in virial equilibrium. As the simulation progresses, turbulence decays through shocks in the core, dissipating kinetic energy. The core then begins to undergo collapse, with density increasing until the formation of individual protostars. The morphology of the cloud is similar in each simulation - the core becomes elongated, generating significant structure which forms the basis for subsequent fragmentation (e.g. Figure 1). All 3 isothermal simulations produced significant numbers of protostars. Table 1 includes the total number of protostars formed, although results cannot be directly compared as some formation was still ongoing.

3.1. *Comparison of isothermal results.*

Figure 1 displays different stages during Models 1 & 2, which apply different power spectra. The main difference between Models 1 & 2 is the timescale for protostar formation and fragmentation. Collapse and protostar formation occur later in Model 1 compared to Model 2, although their overall evolution is similar. This is due to the shallower power law $P \propto k^{-3.5}$ (compared to $P \propto k^{-4}$ for Model 2 when $\alpha = 0.5$) which supplies more kinetic energy over smaller length scales. This provides greater support over small scales and generates more structure. Consequently density plots for Model 1 show more structure than those for Model 2, and the protostars are less widely distributed (Figure 1).

The left side of Figure 1 illustrates the evolution for the $\alpha = 0.25$ dispersion law, which best represents McKee & Tan (2003). There are 2 phases of star formation, at $\approx 0.25 t_{ff}$ and $\approx 0.47 t_{ff}$ which produce a total of 28 protostars after $0.54 t_{ff}$. Initially a protostar forms surrounded by a disc of gas, which then fragments into 2 more protostars. Later fragmentation is predominantly through collapse of elongated filaments. Model 2 (figure 1, right) shows similar behaviour, again with disc fragmenation followed by filamentary fragmentation producing 14 protostars after $0.44 t_{ff}$.

The degree and timescale of fragmentation vary according to both the turbulent power law and the size of the core. Whereas a steeper velocity-sizescale relation ($\alpha = 0.25$) advances protostellar formation, collapse is delayed for the $R = 0.2$pc core in Model 3. The larger core has more thermal support so the ratio of thermal to gravitational energy is greater. Protostar formation begins at $\sim 0.52 t_{ff}$, so collapse of the core and subsequent fragmentation occurs at a higher fraction of the free fall time compared with Model 1 where $R = 0.06$pc. Correspondingly, density plots for Model 3 also show less structure,

Model	α	R (pc)	Jean No.	Predominant time of formation (t_{ff})	No. of protostars	Total mass accreted ($M_{\odot}$)	Most massive protostar ($M_{\odot}$)
1	0.25	0.06	69	0.47	28	2.73	0.435
2	0.5	0.06	69	0.37	14	2.12	0.528
3	0.25	0.2	12	0.55	19	1.79	0.66
4	0.25	0.06	69	0.54	3†	2.02	0.99
5	0.25	0.2	12	0.54	2	2.10	1.28

Table 1. Table showing results of all simulations, giving the total number of stars formed and the approximate time at which most formation occurred. Models 4 & 5 use a non-isothermal equation of state above a critical density (Section 2.2.2). However Model 4 also includes a second isothermal collapse phase. †Further fragmentation apparent but sink formation suppressed by equation of state.

https://doi.org/10.1017/S1743921305004382 Published online by Cambridge University Press

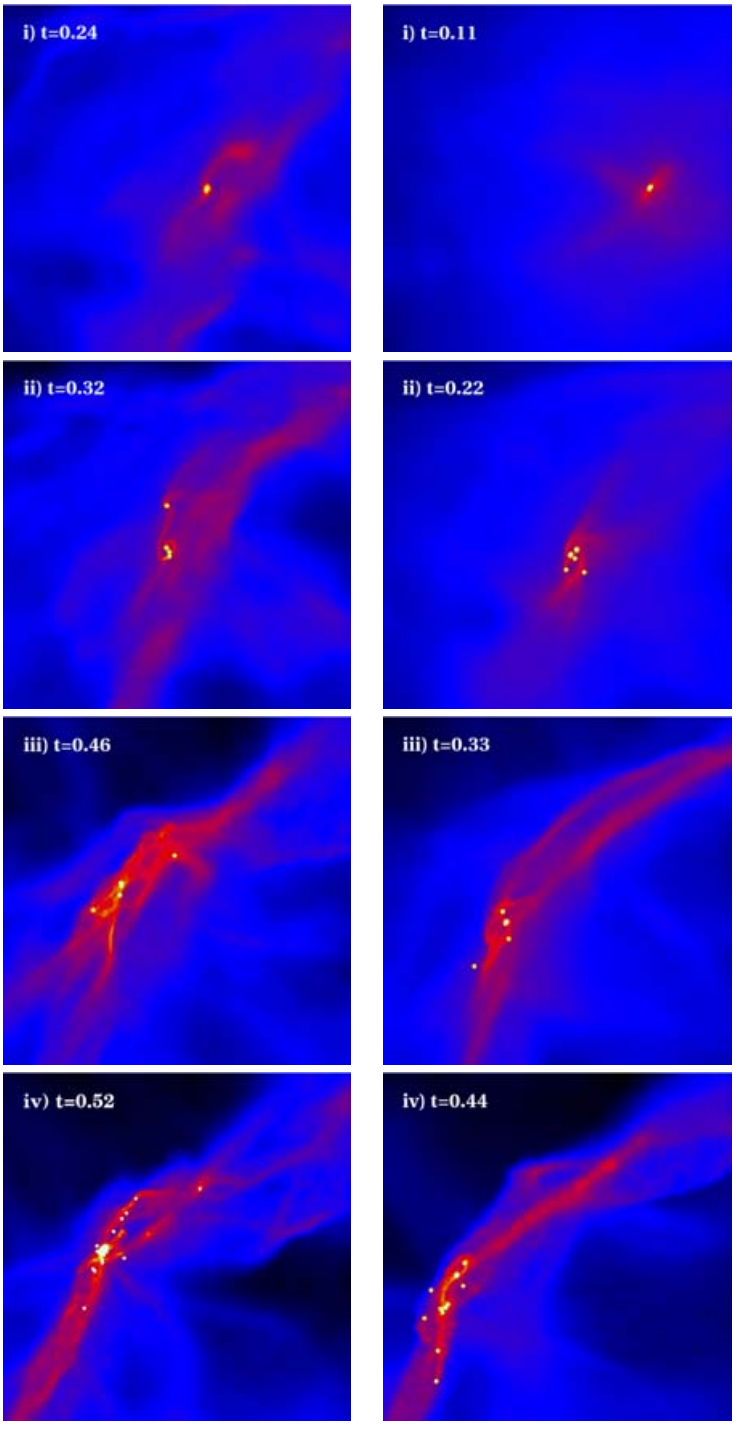

Figure 1. Column density plots (logarithmic scale, minimum and maximum densities of 4×10^{-17}gcm^3 and 4×10^{-13}gcm^3) showing evolution of central region of the core for $\sigma \propto L^{0.25}$ (left) and $\sigma \propto L^{0.5}$ (right). Length scale for each plot is 0.02pc $\times$ 0.02pc. The number of protostars in the plots are: Left - i)1, ii)4, iii)6, iv)24; Right - i)1, ii)7, iii)7, iv)14 . Times are given in units of $t_{ff} = 4.5 \times 10^4$ years.

https://doi.org/10.1017/S1743921305004382 Published online by Cambridge University Press

tending to retain a centrally condensed profile, at least over large length scales. There was, however, still sufficient structure over the centre to produce 19 protostars over $0.6t_{ff}$, so significant fragmentation still occurred.

3.1.1. *Accretion rates*

The main motivation for McKee & Tan (2003) was to achieve a high accretion rate to overcome radiation pressure. Accretion rates can generally be estimated as the resulting protostellar mass divided by the free-fall time (M/t_{ff}). Thus McKee & Tan (2003) construct their models to produce an early accretion rate of $10^{-4}M_{\odot}yr^{-1}$, which increases to $10^{-3}M_{\odot}yr^{-1}$. We find the accretion rate in our results to be initially $\sim 10^{-4}M_{\odot}yr^{-1}$ increasing to $10^{-3}M_{\odot}yr^{-1}$ after $0.3t_{ff}$. These accretion rates agree with McKee & Tan (2003), but are based on the total mass accreted onto many protostars (between ∼5–20). The accretion rate for an individual protostar is therefore significantly less. In contrast, the cluster accretion models for massive star formation (Bonnell, Vine & Bate 2004) show that although the mean accretion rate (M/t_{ff}) is only $10^{-6}M_{\odot}yr^{-1}$, the actual accretion rate onto the growing massive star in the centre of a cluster is $10^{-4}M_{\odot}yr^{-1}$.

3.2. *Non-isothermal results*

The large scale collapse of the non-isothermal models are very similar to the corresponding isothermal cases, since the equation of state changes only in the central denser regions. However, Table 1 shows that the number of protostars formed is dramatically reduced (Models 4 & 5). In Model 4, (0.06pc core), the equation of state changed before fragments could collapse to form sink particles. A second isothermal collapse phase subsequently produced 3 protostars. For Model 5 (0.2pc core), the core is initially less dense so 2 protostars were able to form without any second collapse phase.

On small scales, comparable to the disc in figure 1 (left), the non-isothermal equation of state leads to dense volumes of thermally supported gas. However on larger sclaes, density profiles show that considerable structure still exists. The distortion of the 0.06pc core in particular suggests that monolithic formation is unlikely, despite the formation of very few protostars. Our analysis suggests fragmentation will occur producing at least 6 separate bodies. This is again a consequence of anisotropic turbulence dominating homogeneous thermal support.

4. Conclusions

Centrally condensed turbulently supported clouds have been hypothesised to be the progenitors of massive stars as their concentration could prevent fragmentation and their high accretion rates overwhelm the radiation pressure from the accreting massive star (McKee & Tan 2002, 2003) We have performed numerical simulations of this scenario and found that the initial centrally condensed density profile proved insufficient to prevent fragmentation. Turbulent support generates significant structure in the core which forms the basis for subsequent fragmentation. Turbulence cannot be assumed to act as the equivalent of an isotropic pressure. In addition, although the total mass accretion rates are comparable with McKee & Tan (2003), individual protostellar accretion rates are significantly lower.

These simulations neglect the potential effects of any magnetic fields present in the core. We do note that this should not impede the fragmentation process as magnetic fields have been shown not to affect the structure generation in turbulent molecular clouds (Stone, Ostriker & Gammie 1998, Padoan *et al.* 2004). Even in the presence of

https://doi.org/10.1017/S1743921305004382 Published online by Cambridge University Press

magnetic fields, turbulence does not act as an isotropic support, and neither turbulence nor magnetic fields should be modelled as an isotropic pressure term.

References

Beech, M. & Mitalas, R. 1994, *ApJ* 95, 517
Behrend & Maeder 2001, *A&A*,373,190
Bonnell, I.A. & Bate, M.R. 2002, *MNRAS* 336, 659
Bonnell, I.A., Bate, M.R. & Zinnecker, H. 2002, *MNRAS* 298, 93
Bonnell, I.A., Vine,S.G., & Bate, M.R. 2004, *MNRAS* 349, 735
Carpenter J.M., Meyer M.R., Dougados, C., Strom, S.E., & Hillenbrand, L.A. 1997, *AJ* 114, 198
Clarke, C.J., Bonnell, I.A., & Hillenbrand, L.A. 2000, *Protostars and Planets IV* pp 151-+
Dobbs, C.L., Bonnell, I.A., & Clark, P.C. 2005 *MNRAS* pp 404-+
Hillenbrand, L.A. & Hartmann, L.W. 1998, *ApJ* 492, 540
Lada, C.J., & Lada, E.A. 3002, *A&A* 41, 57
Larson, R.B. 1981, *MNRAS* 194, 809
Mac Low, M.M., Klessen, R., Burkert, A., Smith, M.D., Kessel, O. 1997, *Bulletin of the American Astronomical Society* 29, 1244
McKee, C.F., & Tan, J.C. 2002, *Nature* 416, 59
McKee, C.F., & Tan, J.C. 2003, *ApJ* 585, 850
Myers, P.C. 1983, *ApJ* 270, 105
Padoan, P., Jimenez, R., Juvela, M., & Nordlund, A. 2004, *ApJL* 604, L49
Stone, J.M., Ostriker E.C., & Gammie, C.F. 1998, *ApJL* 508, L99
Wolfire, M.G., & Casinelli, J.P. 1987, *ApJ* 319, 850
Yorke, H.W., & Sonnhalter C. 2002, *ApJ* 569, 846
Zinnecker, H., McCaughrean, M.J. & Wilking, B.A. 1993, *in Protostars and Planets III the initial stellar population* pp 429–495